

LETTER TO THE EDITOR

An enigmatic H I cloud.

L. Dedes¹, C. Dedes², and P.W.M Kalberla¹

¹ Argelander Institut für Astronomie (AIfA), University of Bonn, Auf dem Hügel 71, 53121 Bonn
e-mail: ldedes@astro.uni-bonn.de, pkalberla@astro.uni-bonn.de

² Max-Planck-Institut für Radioastronomie, Auf dem Hügel 69, 53121 Bonn

Received —; accepted —

ABSTRACT

Aims. The discovery of an H I cloud with peculiar properties at equatorial coordinates (J2000) $\alpha=07^h49^m$, $\delta=04^d30'$ is presented.

Methods. The H I object was detected at 21cm using the 300-m NAIC Arecibo* telescope. Subsequent follow-up high-resolution observations with the NRAO Very Large Array** (VLA) telescope at L-Band revealed more details about its morphology.

Results. The most intriguing aspect of the object is the clear velocity gradient of 1 km s^{-1} , which is present in the data, an indication of either rotation or expansion. The gas appears to be cold, and its morphology is somewhat elliptical with clumpy substructure. Assuming disk rotation, the dynamical mass could be determined as a function of distance.

Conclusions. Depending on the exact nature of the velocity gradient in the H I cloud, we can reach some preliminary conclusions about the nature of the object. Expansion would imply association with a circumstellar envelope of an evolved AGB star, while in the case of rotation, a comparison between the visible and the dynamical mass can lead to some preliminary conclusions. A common feature of those conclusions is the presence of a gravitational potential well, which is required to account for the rotation of the trapped H I gas. This potential well could be associated with a dark galaxy or some other exotic object.

Key words. ISM: structure - Galaxy: halo - Radio lines: general

1. Introduction

During the past decade, the introduction of new state-of-the-art instruments like the new ALFA multi-pixel receiver of the Arecibo telescope and a superb H I all sky survey i.e. the Leiden/Argentinian/Bonn (LAB) survey (Kalberla et al. 2005) has led to a renaissance in Galactic H I astronomy. In this context, we used the Arecibo 300-m Radio-telescope to survey a field of $17^\circ \times 5^\circ$ at (l,b) \sim (218°, 15°) in the sky for H I halo clouds (Dedes et al; in prep.) with properties similar to the ones detected by the GBT 100-m telescope (Lockman 2002). During these observations, an H I cloud with peculiar properties was detected.

In this short letter we would like to report its properties and discuss its nature. The layout is the following. In Sect. 2, the single dish Arecibo and the VLA observations are discussed, in Sect. 3, the observational properties of the H I cloud presented, and in Sect. 4, possible interpretations regarding the nature of the cloud discussed.

2. Observations

The H I line observations at the Arecibo telescope were done during August 2006. As front-end, the ALFA multi-beam receiver was used at a wavelength of 21cm in conjunction with the GALSPECT spectrometer, which has a bandwidth of 7.14 MHz and 8192 channels. An area of $17^\circ \times 5^\circ$ was mapped

around the coordinates $\alpha=08^h00^m00'$, $\delta=02^d45'00''$. The Arecibo data were reduced using the IDL routines developed by C. Heiles and J. Peek (Stanimirović et al. 2006). The result was an image cube with an angular resolution of $\sim 4'$ and a velocity resolution of 0.18 km s^{-1} .

The follow-up observations of the cloud took place in July 2008 at the VLA. The H I cloud was observed for ~ 6 hours in the L-band with the array in D-configuration. A single IF was used as backend with a bandwidth of 781 kHz and 512 channels. With this configuration we have a channel separation of 1.5 kHz and a velocity separation of 0.3 km s^{-1} . This is the narrowest possible bandwidth to use for avoiding the aliasing appearing in the EVLA-EVLA baselines when using a combination between the 11 VLA and the 16 new EVLA antennas.

The data were reduced using the AIPS¹ package, including the task FXALIAS to correct the aliasing in the EVLA-EVLA baselines. As a flux calibrator, the source 0137+331 was used, while the close-by source 0739+016 was taken as a phase calibrator. The dirty cube had an rms noise of $\sim 5\text{ mJy/beam}$. After applying a continuum subtraction, the dirty cube was deconvolved using the CLEAN Clark algorithm (Clark 1980).

The cloud was also observed with the 295 channel Large Bolometer Camera (LABOCA) (Siringo et al. 2007) at the Atacama Pathfinder Experiment (APEX²) telescope during August and December of 2007. LABOCA operates at $870\mu\text{m}$ with an angular resolution of $19''$. The total time spent on source

* The Arecibo Observatory is part of the National Astronomy and Ionosphere Center, which is operated by Cornell University under a co-operative agreement with the National Science Foundation

** The National Radio Astronomy Observatory is a facility of the National Science Foundation operated under cooperative agreement by Associated Universities, Inc.

¹ http://www.aips.nrao.edu/aips_faq.html

² APEX is a collaboration between the Max-Planck-Institut für Radioastronomie, the European Southern Observatory, and the Onsala Space Observatory.

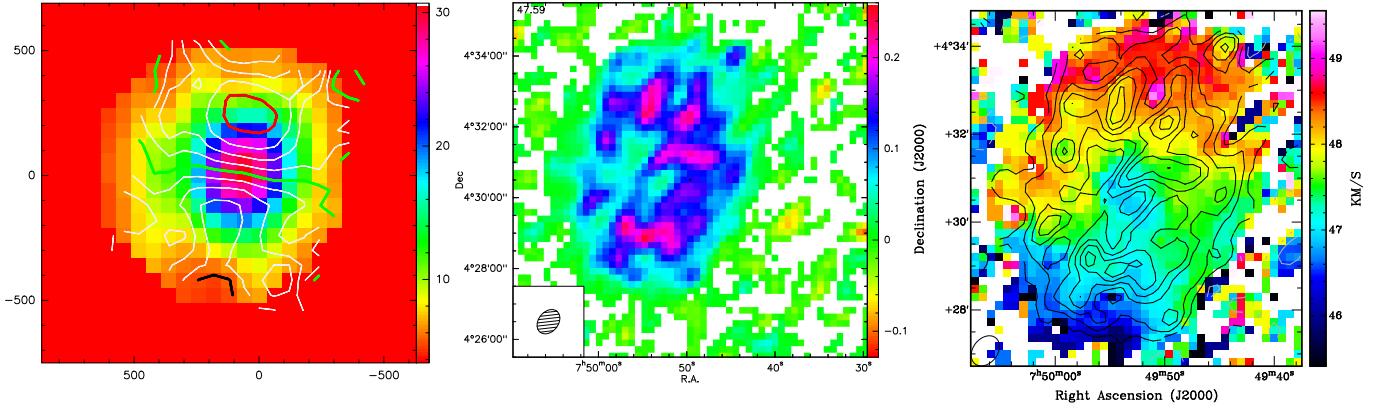


Fig. 1. Left: a) A 0 moment map of the Arecibo data showing the H I cloud. Emission outside the object was blanked. The transfer function is linear with units of Kkm s^{-1} . As contours, the 1st moment map is over-plotted. The contour levels are from $v_{lsr}=47.2\text{km s}^{-1}$ (black) to $v_{lsr}=48.00\text{km s}^{-1}$ (red) in steps of 0.1km s^{-1} , with 47.6km s^{-1} marked as a green contour. Middle: b) A 0-moment map of the VLA observation. The transfer function is linear. The units are in Jy/Beam km s^{-1} . Right: c) A 1st moment map of the VLA observation, depicting velocity from 45.4km s^{-1} to 49.6km s^{-1} in step of 0.3km s^{-1} . The 0 moment has been overlaid as a contour map with contour levels from 10% up to 90% of the peak with a step of 10%.

was 1.5 hours, reaching an rms of 5 mJy/beam with an average zenith opacity of 0.2 at $870\mu\text{m}$. The data were reduced using the LABOCA reduction package BOA (Schuller et al., in prep).

3. Results

3.1. Arecibo

In the Arecibo data, a spherical H I object with an average angular size of $6.4'$ at $\alpha=07^{\text{h}}49^{\text{m}}49.613''$ and $\delta=04^{\circ}30'30''$ with a $v_{lsr}=47.6\text{km s}^{-1}$ was detected. It has a column density of $N_{\text{peak}} = 60 \times 10^{18} \text{ cm}^{-2}$ and average $\Delta v_{1/2}$ line width of $3.4 \pm 0.18\text{km s}^{-1}$. Figure 1a) shows a zero-moment map at the position of the clump with the 1st moment map overlaid as contours. The contours of the velocity field close to the peak of the emission show a velocity gradient of $0.8 \pm 0.18\text{km s}^{-1}$ for the H I object. The parallel lines of the velocity field can be interpreted as a signature of a rotating disk or a uniform expanding shell. While the spectral resolution is very good, the angular resolution is not good enough to provide more information.

3.2. VLA results

The VLA observations confirmed the detection of the velocity gradient of the H I cloud seen with the Arecibo telescope and gave more information regarding the spatial structure of the object.

In the consecutive channel maps shown in Fig 2, the velocity gradient in the cloud is clearly seen. The high-resolution observations revealed a number of interesting features in the object:

- In the 0-moment map shown in Fig.1 b), the object has an elliptical shape in contrast to the spherical shape shown in the Arecibo data. The region where H I emission is present can be fitted with an ellipse of major axis $A = 330 \pm 20''$, minor axis $B = 230 \pm 14''$, and position angle $p.a = -14 \pm 7^\circ$. In the 1st-moment map in Fig.1c, the velocity field of the H I cloud is similar to a disk-like object rotating as a solid body. The same result is also inferred when the task *Velfit*

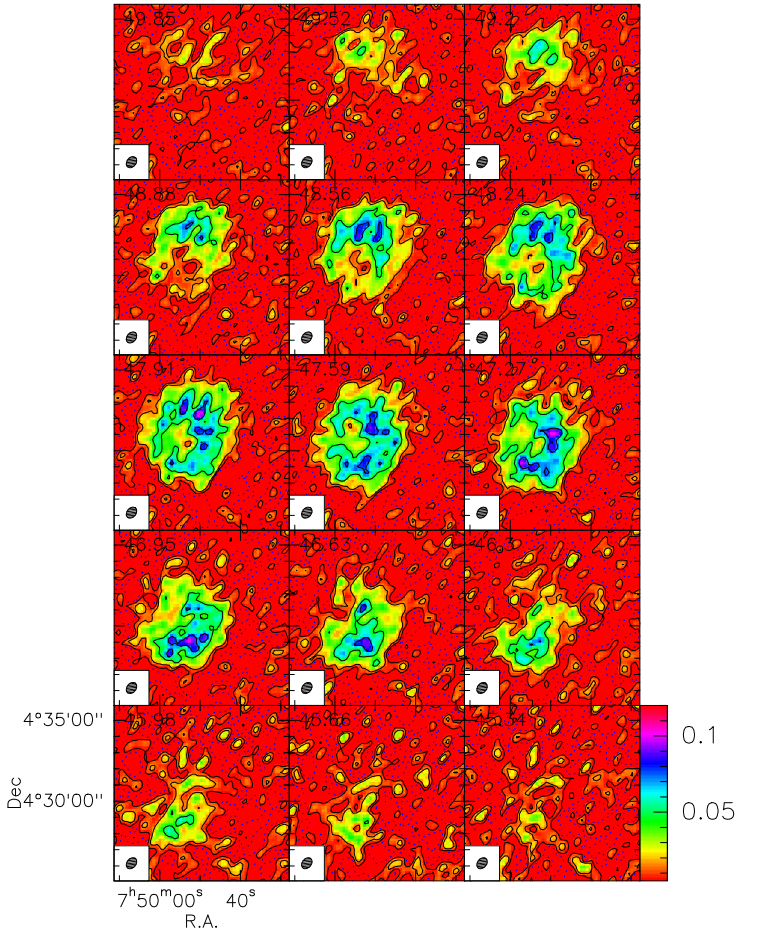


Fig. 2. Series of channel maps for the VLA data from $v_{lsr}=49.85\text{km s}^{-1}$ to $v_{lsr}=48.34\text{km s}^{-1}$. The color scale is r from from 5mJykm s^{-1} to 120mJykm s^{-1} with a linear transfer function. The contour levels are plotted from -1σ onwards in steps of $1\sigma, 3\sigma, 9\sigma, 15\sigma, 21\sigma$.

of MIRIAD³ is used to extract a rotation curve from the 0

³ <http://www.atnf.csiro.au/computing/software/miriad/>

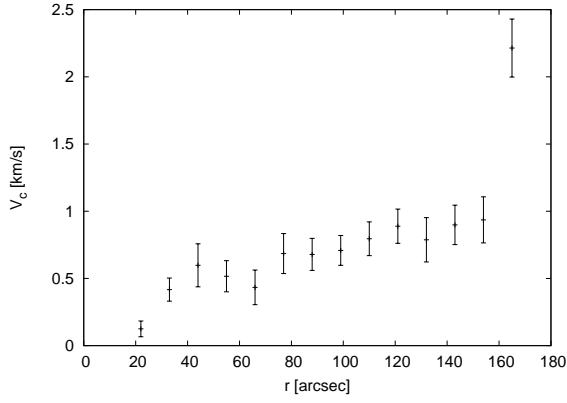


Fig. 3. The rotation curve of the H I cloud as extracted using the 0-moment and the 1st-moment maps. V_c is the circular velocity in km s^{-1} , r the radius of the clouds from the center, in arcseconds.

moment and the 1st-moment maps of the H I cloud. This is seen in Fig. 3. Nevertheless, the D-configuration data do not have enough spatial and spectral resolution to model the cloud and exclude expansion sufficiently. The total velocity gradient over the cloud is $2 \pm 0.3 \text{ km s}^{-1}$, which would imply an apparent rotational or expansion velocity of $\sim 1 \text{ km s}^{-1}$.

- From the 0-moment map in Fig. 1b), it can be seen that the H I gas does not have a uniform distribution, which is also seen from the channel maps in Fig. 2. The gas has a shell-like filamentary structure, with several bright peaks. Those have peak column densities from $1 \times 10^{20} \text{ cm}^{-2}$ to $1.8 \times 10^{20} \text{ cm}^{-2}$. The filaments must be very cold, since they have a line width $\Delta v_{1/2} \sim 2.3 \text{ km s}^{-1}$. The H I emission contained in the peaks can be used to calculate the total visible H I mass. Assuming that the system is at a distance d and is optically thin, the total visible H I mass as a function of distance, using the average column density for each of the peaks, is given by

$$\frac{M_{\text{HI}}}{M_{\odot}} = 7 \cdot 10^{-7} \cdot \frac{d^2}{\text{pc}^2}. \quad (1)$$

- In the comparison between the 0-moment and the 1-st moment maps in Fig. 1 c), the last important feature is revealed. At position $\alpha = 07^{\text{h}}49^{\text{m}}53^{\text{s}}$, $\delta = 04^{\text{d}}30'19''$, there is a column density minimum with $N_{\text{HI}} = 3 \times 10^{19} \text{ cm}^{-2}$ at the same position where there is a discontinuity in the velocity field. This apparent hole in the emission seems to be close to the center of rotation.

3.3. Dynamical Mass

If the velocity field seen in Fig. 1 c) can be attributed to a rotating disk following solid-body rotation, the dynamical mass can be estimated easily. We assume an apparent rotational velocity $\sim 1 \text{ km s}^{-1}$, a disk of inclination $i \sim 45^\circ$, and an angular radius of $s = 165''$. At a distance of d , the dynamical mass is

$$\frac{M_{\text{tot}}}{M_{\odot}} = 0.37 \cdot \frac{d}{\text{pc}}. \quad (2)$$

Assuming a uniform rotating disk, the above equation implies an angular momentum $J = 1.3^{46} \times (d/\text{pc})^2 \text{ m}^2 \cdot \text{kg/s}$. The

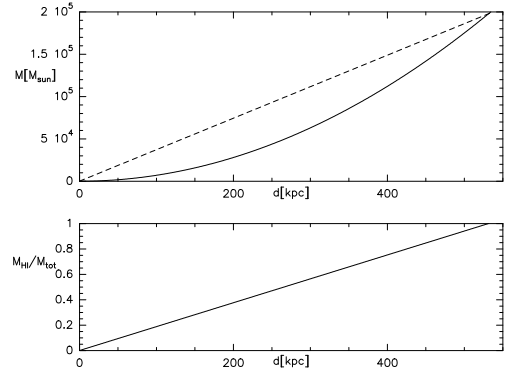


Fig. 4. Top : A diagram comparing the total visible H I mass M_{HI} (black line) of the cloud measured from the VLA data and the dynamical mass M_{tot} (dashed line) as a function of distance d (kpc). Bottom : Diagram giving the ratio of the $M_{\text{HI}}/M_{\text{tot}}$ of the cloud as a function of distance d (kpc).

distance where the dynamical mass M_{tot} is equal to the visible H I mass is $d_m = 530 \text{ kpc}$. This implies a total mass of $M_{\text{tot}} = 1.97 \times 10^5 M_{\odot}$ and a diameter of 850 pc . In Fig. 4, a comparison between the visible H I mass and the dynamical mass is shown. For any distance smaller than d_m , the estimated dynamical mass is significantly greater than the total observed H I mass. As an example, if the cloud is located at a distance of 50 kpc , this would imply that only 10% of the total mass is in H I. In such a case the dynamical mass would be $M_{\text{tot}} = 1.8 \times 10^4 M_{\odot}$ and its diameter only 80 pc .

3.4. Comparison with data at other wavelengths

The 0 moment map of the H I VLA observations was also compared with observations at different wavelengths. The dust continuum observations conducted with APEX as part of this work show no detection of cold dust above the rms of 5 mJy/beam and attempts during the data reduction to recover possible faint extended emission were unsuccessful. Assuming a dust-to-gas ratio of $1/150$ (Klein et al. 2005), $\beta = 2$ (Priddey & McMahon 2001) and $k_v(\nu) = 0.04 \times (\nu/250 \text{ GHz})^\beta$ (Kruegel & Siebenmorgen 1994), an upper limit for the H_2 column density is $N_{\text{H}_2} = 9 \times 10^{20} \text{ cm}^{-2}$. It has to be taken into account that the dust parameters are hard to constrain, since the location of the cloud is not known and average disk values were taken for the calculation. Assuming e.g. a 10 times lower dust-to-gas ratio to reflect changing metallicities in the halo (Wakker 2001), the column density would change accordingly.

In addition, utilizing the NED⁴, HEASARC⁵, SKYVIEW⁶ and IRSA⁷ databases, the 0 moment map was compared with the publicly available surveys at various wavelengths. No obvious correlation was found except from the 2MASS survey (Skrutskie et al. 2006), where a star was found at coordinates

⁴ This research has made use of the NASA/IPAC Extragalactic Database (NED), which is operated by the Jet Propulsion Laboratory, California Institute of Technology, under contract with the National Aeronautics and Space Administration.

⁵ <http://heasarc.gsfc.nasa.gov/>

⁶ <http://skyview.gsfc.nasa.gov/>

⁷ This research has made use of the NASA/ IPAC Infrared Science Archive, which is operated by the Jet Propulsion Laboratory, California Institute of Technology, under contract with the National Aeronautics and Space Administration.

(J2000) $\alpha=07^h49^m53.51''$, $\delta=04^d30'23.69''$. This is exactly the location where the hole, i.e the drop in the column density of the 0 moment map is found. The apparent K, H, and J magnitudes are 10.225, 10.237, 10.504, respectively.

4. Discussion

From the observational results presented above, four main characteristics of the H I cloud can be identified, which, if intrinsic, can give us an insight regarding the nature of the object: a) the H I cloud exhibits a velocity gradient of $\sim 2\text{km s}^{-1}$. While the velocity field is compatible with solid-body rotation, based on the VLA data expansion cannot be excluded. b) The overall structure as seen in Fig.1 c) of the H I cloud is elliptical. c) The structure as seen in Fig.1 b) is rather filamentary with a hole in the middle of the 0 moment and the 1st-moment map. d) No correlation with any emission in other wavelengths was found except in the 2MASS data, where a star was identified in the hole region. One has to do spectroscopy on the star to rule out a projection effect. Based on the above observations and depending on the distance, the nature of the H I cloud can be interpreted in several ways:

1. Placed at a distance of $d_m \sim 530\text{kpc}$, and assuming rotation, it could be a self-gravitating H I disk. However, the filamentary structure of the cloud excludes this notion as does the difficulty to form such a system and confine the gas into a disk-like structure. The visible H I mass in each filament ranges from $\approx 9 \cdot 10^{-8} \times (d/(\text{pc}))^2 M_\odot$ down to $8 \cdot 10^{-9} \times (d/(\text{pc}))^2 M_\odot$, while the virial mass, assuming a dispersion similar to the line width of 2.3km s^{-1} , is $M_v \sim 1.29 \times d/(\text{pc})$. As a result, in order for the filaments to be self-gravitating, the object would have to be in far greater distance than 530kpc , but in such a distance, their total mass would be greater than the one required for the apparent rotation.
2. For any distance $d < d_m$, as seen in Fig. 4, the total visible H I gas cannot account for the observed rotation. In such a case, the neutral hydrogen plays the role of a tracer of gravitational potential. The mass responsible for such a gravitational potential would range from a few hundred solar masses at a distance shorter than one kpc up to $4 \times 10^4 M_\odot$ at a distance of 100kpc .

Placed at a distance of about 50kpc , typical for satellites like the Magellanic Clouds (Cioni et al. 2000), the object would have dimensions similar to dwarf galaxies (e.g Sgr dwarf, for $d=20\text{kpc}$ [Monaco et al. 2004] the radius is $r \sim 30\text{pc}$). The associated mass in such a case would be lower than a typical dwarf galaxy mass, which, using the arguments of Jimenez et al. (1997) might indicate that the mass is too low to initiate star formation. It has to be noted that the dynamical mass obtained could be only a lower limit on the true mass, since it takes into account the rotation of the visible H I gas, therefore underestimating a possible contribution of dark matter extending past the radius of the visible mass. It looks as though the object exhibits properties of the dark galaxy population that is expected to be present in the Milky Way halo (Jimenez et al. 1997). These authors also claim that such an object should be detected in empty fields within deep H I surveys, as was the case with the data presented here. The object is isolated in the Arecibo data, blended only with background faint emission of Galactic origin. Another sign for the association of the H I object

with a galaxy is the extreme morphological similarity the object shows with the atomic gas disk of the Galactic bulge discussed in Ferrière et al. (2007).

3. At a distance greater than 530kpc , the visible mass would exceed the dynamical mass. In such a case, the visible mass would not be gravitationally bound and one would not expect to observe such a rotational profile.
4. Discussion about a more exotic object like a black hole would require studying the object in tracers such as X-ray emission.
5. In the above cases, the apparent velocity gradient was explained as a result of solid body rotation, but this is not the only feasible explanation. Assuming that the H I cloud has a distance of 400pc (i.e average distance of circumstellar envelopes from Gérard & Le Bertre 2006), it would then have a diameter of $D=0.53\text{pc}$, an H I mass $M_{\text{vis}} = 0.11 M_\odot$, and an expansion velocity of $\sim 1\text{km s}^{-1}$. All three parameters agree well with the ones found in the H I survey of circumstellar envelopes around evolved stars (Gérard & Le Bertre 2006). In such a case, the H I cloud could form a shell due to mass loss from the star detected in the 2MASS survey. Possible detection of molecular gas in the H I cloud would further support this option, since most of the envelopes in Gérard & Le Bertre (2006) are associated with CO emission.

Nevertheless, it is difficult to reach an irrefutable conclusion regarding the nature of the object. More observations are needed, i.e deep synthesis 21-cm line observations to accurately determine the extent of the H I disk and to distinguish between expansion and rotation, optical observations to clarify possible association of the star in the 2MASS survey with the H I cloud, and observations of CO to determine a possible molecular content of the cloud.

Acknowledgements. Leonidas Dedes was supported by the German *Deutsche Forschungsgemeinschaft*, DFG project number KA1265/5-1. L. Dedes would like to thank S. Stanimirovic, J. Peek, and K. Douglas for their help with the Arecibo data reduction. C. Dedes was supported by the Studienstiftung des Deutschen Volkes and is a member of the International Max Planck Research School (IMPRS) for Astronomy and Astrophysics. The authors would like to thank Miguel Requena-Torres for his useful corrections. The authors would like to thank the anonymous referee for the helpful comments.

References

- Cioni, M.-R. L., van der Marel, R. P., Loup, C., & Habing, H. J. 2000, *A&A*, 359, 601
- Clark, B. G. 1980, *A&A*, 89, 377
- Ferrière, K., Gillard, W., & Jean, P. 2007, *A&A*, 467, 611
- Gérard, E. & Le Bertre, T. 2006, *AJ*, 132, 2566
- Jimenez, R., Heavens, A. F., Hawkins, M. R. S., & Padoan, P. 1997, *MNRAS*, 292, L5
- Kalberla, P. M. W., Burton, W. B., Hartmann, D., et al. 2005, *A&A*, 440, 775
- Klein, R., Posselt, B., Schreyer, K., Forbrich, J., & Henning, T. 2005, *ApJS*, 161, 361
- Kruegel, E. & Siebenmorgen, R. 1994, *A&A*, 288, 929
- Lockman, F. J. 2002, *ApJ*, 580, L47
- Monaco, L., Bellazzini, M., Ferraro, F. R., & Pancino, E. 2004, *MNRAS*, 353, 874
- Priddey, R. S. & McMahon, R. G. 2001, *MNRAS*, 324, L17
- Siringo, G., Weiss, A., Kreysa, E., et al. 2007, *The Messenger*, 129, 2
- Skrutskie, M. F., Cutri, R. M., Stiening, R., et al. 2006, *AJ*, 131, 1163
- Stanimirović, S., Putman, M., Heiles, C., et al. 2006, *ApJ*, 653, 1210
- Wakker, B. P. 2001, *ApJS*, 136, 463